Biogeochemistry (2008) 88:31–46
DOI 10.1007/s10533-008-9192-9

ORIGINAL PAPER

Nitrogen retention in the hyporheic zone of a glacial river in interior Alaska

Hannah M. Clilverd · Jeremy B. Jones Jr · Knut Kielland

Received: 28 May 2007 / Accepted: 27 February 2008 / Published online: 27 March 2008

Abstract We examined the hydrologic controls on nitrogen biogeochemistry in the hyporheic zone of the Tanana River, a glacially-fed river, in interior Alaska. We measured hyporheic solute concentrations, gas partial pressures, water table height, and flow rates along subsurface flowpaths on two islands for three summers. Denitrification was quantified using an in situ $^{15}NO_3^-$ push–pull technique. Hyporheic water level responded rapidly to change in river stage, with the sites flooding periodically in mid−July to early−August. Nitrate concentration was nearly 3-fold greater in river (ca. 100 μg NO_3^-–N l^{-1}) than hyporheic water (ca. 38 μg NO_3^-–N l^{-1}), but approximately 60–80% of river nitrate was removed during the first 50 m of hyporheic flowpath. Denitrification during high river stage ranged from 1.9 to 29.4 mg N kg sediment^{-1} day^{-1}. Hotspots of methane partial pressure, averaging 50,000 ppmv, occurred in densely vegetated sites in conjunction with mean oxygen concentration below 0.5 mgO_2 l^{-1}. Hyporheic flow was an important mechanism of nitrogen supply to microbes and plant roots, transporting on average 0.41 gNO_3^-–N m^{-2} day^{-1}, 0.22 g NH_4^+–N m^{-2} day^{-1}, and 3.6 g DON m^{-2} day^{-1} through surface sediment (top 2 m). Our results suggest that denitrification can be a major sink for river nitrate in boreal forest floodplain soils, particularly at the river-sediment interface. The stability of the river hydrograph and the resulting duration of soil saturation are key factors regulating the redox environment and anaerobic metabolism in the hyporheic zone.

Keywords Denitrification · Hyporheic · Methane · Nitrogen · River · Taiga

H. M. Clilverd (✉) · J. B. Jones Jr · K. Kielland
Institute of Arctic Biology, University of Alaska Fairbanks, 211 Irving 1, Fairbanks, AK 99775, USA
e-mail: fthmc1@uaf.edu

Introduction

The hyporheic zone is the saturated sediments beneath and adjacent to rivers and streams, and functions as an ecotone between aquatic and terrestrial environments (Triska et al. 1993; Boulton et al. 1998. As such, the aquatic-terrestrial interface is an active site of biogeochemical transformations, regulating the flux of nutrients between ecosystems (Triska et al. 1989; Jones et al. 1995a; Hedin et al. 1998; Dahm et al. 1998; Baker and Vervier 2004). A strong redox gradient largely driven by hydrological transmissivity and residence time of hyporheic water can occur at this interface within a short distance (e.g., <1 m) of surface water entering the hyporheic zone (Hedin et al. 1998). The supply of electron donors and acceptors to hyporheic sediments drives microbially-mediated, redox-sensitive reactions such as aerobic respiration, nitrification, denitrification, sulfate reduction, methanogenesis, and methane

oxidation (Grimm and Fisher 1984; Holmes et al. 1996; Duff and Triska 2000; Hill et al. 2000; Morrice et al. 2000; Ostrom et al. 2002).

Nitrate retention, in particular, is of interest in near-river environments as hyporheic sediments can mediate the supply of nitrogen from aquatic to terrestrial environments (Lowrance et al. 1984; Jones and Holmes 1996; Hedin et al. 1998; Hill 2000; Schade et al. 2002; Sabater et al. 2003; Vidon and Hill 2004). Nitrate assimilation by plants and removal via denitrification can be influenced by periods of flooding that saturate the rooting zone and alter the local redox environment. Hydrologic exchange as a pathway for nutrient retention is maximized in sinuous, unconstrained rivers (Dahm et al. 1998; Malard et al. 2006). The diverse fluvial geomorphology of braided glacial rivers likely drives strong river-floodplain connectivity. Moreover, this connectivity of glacial rivers can be temporally variable as channel width can vary over 200 m from baseflow to high flow conditions with seasonal changes in discharge.

In glacially fed rivers, river hydrology, and the subsequent effect on hyporheic biogeochemistry, is largely controlled by regional climate and rate of glacial melt. Increased thinning of glaciers in interior Alaska (Arendt et al. 2002) due to climatic warming is predicted to lead to increased frequency and magnitude of flooding (Hinzman et al. 2005). Rising river level can lead to enhanced river water intrusion into the hyporheic zone, prolonging anoxia, and increased supply of dissolved organic carbon and nitrate to subsurface biota, thus increasing floodplain metabolism (Meyer 1988; Findley 1995).

We examined the effects of river stage on hyporheic-zone biogeochemistry in a glacially-fed river in interior Alaska. We addressed the following research questions at two early successional stage floodplain islands: (1) how does the biogeochemistry of hyporheic water change along subsurface flowpaths, and (2) how does temporal variation in glacial melt and river discharge regulate floodplain anaerobic respiration and the supply of nutrients to floodplain vegetation? We predicted that microbially-mediated reduction of hyporheic nitrate would be greatest at the river-sediment interface. Second, we predicted that prolonged saturation of the sediment profile during summer peaks in glacial melt and river discharge would lead to increased anoxia of floodplain sediment, and greater anaerobic respiration.

Methods

Study site

The study was conducted on two islands of the Tanana River located approximately 20 km southwest of Fairbanks, Alaska (64°51′ N, 147°43′ W; elevation ca. 120 m) within the Bonanza Creek Long Term Ecological Research site (Fig. 1). The climate is continental with temperature extremes that range from −50°C to + 30°C. Average daily temperature ranges from −24.9°C in January to +16.4°C in July, with an average annual temperature of −3.3°C (Viereck et al. 1993a). Annual precipitation in the region is low (ca. 270 mm), and is exceeded by potential evapotranspiration (ca. 470 mm). As a consequence, salt precipitates on exposed floodplain soil surfaces in the summer (Viereck et al. 1993a). The Tanana River is a major tributary to the Yukon River. The Tanana River is nearly 1,000 km in length, flowing northwest from glacial headwaters in the Alaska Range (85% of total annual discharge of the Tanana River), and draining a basin of about 113,920 km^2 (Anderson 1970). The Tanana Valley consists of glaciofluvial sediments and alluvial fans, deposited from Tanana River glacial waters and groundwater fed streams that drain from the Yukon-Tanana Uplands that bound the river to the north. Downstream of Fairbanks, the Tanana River valley opens to 80–100 km in width, and has an active floodplain of 300–2,000 m across (Anderson 1970). Sedimentary deposits on the Tanana River floodplain can be over a 100 m thick (Péwé et al. 1976, Péwé and Reger 1983); as a consequence, geochemistry of floodplain soil is governed by weathering of exogenous sediments rather than the local parent material.

Floodplain soil is a mixture of alluvial deposits that vary from sand to silt-loam across primary successional stages (Viereck et al. 1993b). Newly deposited silt is first colonized by communities of willow (*Salix* spp.) and horsetail (*Equisetum* spp.). Alder (*Alnus tenuifolia*)/willow stands develop with increasing distance from the river, followed by balsam poplar (*Populus balsamifera*), white spruce (*Picea glauca*) and finally black spruce (*P. mariana*). A more detailed description of the climate and vegetation on the Tanana River floodplain is given by Viereck et al. (1993a, b).

At the study sites the Tanana River forms of a series of braided channels with sandbars and islands.

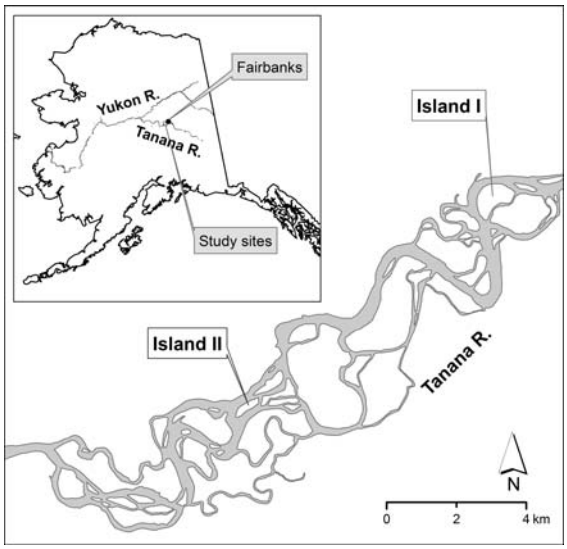

Fig. 1 Location of the two study islands on the Tanana River, approximately 20 km southwest of Fairbanks, Alaska

The two study islands were approximately 1 km wide and 1–2 km in length, and as replicates they were chosen for their similar geomorphology and vegetation type. We focused our research on recently deposited alluvium (<10 years old), where vegetation is dominated by willow. An organic soil horizon was absent and, as a consequence, soil organic carbon and nitrogen standing stocks were very low (Viereck et al. 1993b; Kielland et al. 2006). Permafrost is generally absent under the riverbed and the adjacent alluvium, but develops in later successional stages as vegetative cover increases (Yarie et al. 1998). The soil water chemistry is dominated by calcium and magnesium, and is moderately basic (pH 7–8). Atmospheric N deposition is low with a mean wet N deposition <0.09 g N m^{-2} yr^{-1} (National Atmospheric Deposition Program, 2003–2005).

Study design

We examined spatial variation in subsurface biogeochemistry by (1) installing well transects to determine water table height and flow velocity, (2) measuring hyporheic solute and gas concentrations, (3) measuring in situ denitrification, and (4) calculating nitrogen flux along hyporheic flowpaths. We installed well transects (one transect per island) approximately 1 km in length across the two islands. Seven to nine wells per island were aligned parallel to the predicted hyporheic flow direction, extending all the way across the islands at intervals of 70 m at Island I and 100 m at Island II. Measurements of hydraulic head along the well transect were used to determine the direction of hyporheic flow. Additional wells were installed lateral to each well transect to determine the slope of hyporheic water surface from hydraulic head measurements. Wells were 3 m long (3.8 cm diameter), with 2 m of the wells below the sediment surface, and the bottom of the wells were approximately 1 m below the average annual minimum water table height. The wells were made from PVC pipe, with the lower 1.5 m being perforated (3 mm diameter holes) and wrapped in geotextile cloth to prevent blockage with fine silts (apparent opening size = 0.2 mm). The tops were covered with PVC caps between sampling dates.

Sampling and analytical techniques

We sampled wells every 2 weeks over the growing season (June–September) for 3 years (2003–2005). Before sampling, wells were purged to introduce fresh hyporheic water. At the time of sampling the water height in each well was measured. Water and gas samples were collected using a peristaltic pump and Tygon tubing (6.4 mm ID), and stored in 100 ml polyethylene bottles and 30 ml syringes, respectively. Sample bottles and syringes were acid-washed and rinsed with deionized water prior to use. Samples were stored in a cooler until return to the laboratory, refrigerated, and then filtered within 24 h. Water samples that could not be analyzed within a week of collection were frozen.

We analyzed cations (Ca^{2+}, Mg^{2+}, K^+, Na^+, NH_4^+) and anions (SO_4^{2-}, Cl^-, NO_3^-, NO_2^-, PO_4^{3-}, Br^-) on a Dionex DX-320 ion chromatograph. Total dissolved nitrogen (TDN), dissolved organic carbon (DOC) and dissolved inorganic carbon (DIC) were determined using a Shimadzu TOC-5000 analyzer plumbed to an Antek 7050 nitric oxide chemoluminescent detector. We calculated dissolved organic nitrogen (DON) as the difference between TDN and dissolved inorganic nitrogen (DIN). Gases (CH_4, CO_2, N_2O) were extracted from syringe samples by headspace equilibration with helium (see method in Jones and Mulholland 1998a) and measured using a Varian CP-3800 gas chromatograph the day after

collection. Electrical conductance was measured using an Accument portable ASPSO conductivity meter, pH was measured using a Beckman-390 pH meter, and dissolved oxygen was quantified in situ using a YSI-55 meter. We calculated bicarbonate concentration using the USGS aqueous geochemical model PHREEQC (Parkhurst and Appelo 1999) using measured ion concentrations, DIC, pH and pCO_2.

Water extractable cations were measured in the laboratory to examine the coupling between sediment cation exchange and hyporheic water chemistry. In the field, floodplain sediments were collected from 28 points at a depth of 100 cm. In the laboratory, 100 ml of deionized water was mixed with 10 g of sediment and placed on a mixing table for 24 h (method amended from Robertson et al. 1999). Following extractions, water was filtered and analyzed as above. The results from the water extractions were compared with river and hyporheic water chemistry as percent composition of total cations using a ternary plot to standardize differences in the absolute concentrations between samples collected in the field and cation exchange estimated in the laboratory.

Subsurface flow rate was measured using dilution gauging of a conservative tracer (15 g NaCl l^{-1}) injected into hyporheic wells (n = 10 wells total). After adding salt, wells were mixed using a miniature gear pump to continuously circulate water. We measured the decrease in electrical conductance of the well water every 5 min for a minimum of 1 h. We calculated subsurface flow rate (υ; m day^{-1}) from the decline in electrical conductance over the sample time as

$$\upsilon = \frac{V_{well} r}{A_{well}} \quad (1)$$

where V_{well} is the volume of the well (m^3), r is the decay constant (day^{-1}), and A_{well} is the cross-sectional area of the well exposed to flow (water depth × well diameter; m^2). The decay constant r was solved by fitting a regression line to the following equation

$$r = \ln \frac{\left(\frac{C_i}{C_0}\right)}{t} \quad (2)$$

where C_i is the electrical conductance at time i, C_0 is the intial electrical conductance, and t is time (day).

We calculated hydraulic conductivity assuming Darcian flow as

$$K = \frac{(\upsilon \eta)}{\left(\frac{\Delta h}{\Delta l}\right)} \quad (3)$$

where K is hydraulic conductivity (m min^{-1}), η is effective porosity. We calculated η from the difference in the volume of saturated and dry sediment collected from 0 to 20 cm depths, $\Delta h/\Delta l$ is the water table slope and was obtained from hydraulic head measurements taken at each well along the transect, and υ is flow rate in (m day^{-1}; Freeze and Cherry 1979).

In situ denitrification

Hyporheic denitrification rate was measured at both island sites using an in situ push–pull ^{15}N–NO_3^- technique (Addy et al. 2002, Baker and Vervier 2004). This method used a conservative tracer (NaBr) and enriched $^{15}NO_3^-$ dosing solution to measure denitrification rate in wells without disturbing sediments. We measured denitrification rates every 2 weeks from June to September in 2005. First, we inserted suspended bladders, spaced 0.2 m apart, into wells to isolate a section that was 1.8 m below the sediment surface (volume of isolated section = 0.23 l; Fig. 2). Then, we used a peristaltic pump to extract (pull) 20 l of hyporheic water into a collapsible cubitainer. This volume of sample pulled water from a sediment volume of approximately 38 l. The pulled water was amended with a $\delta^{15}NO_3^-$ and NaBr solution. The nitrate concentration in the cubitainer was elevated approximately 20% above background (background = 33 μg l^{-1} of $^{14}NO_3^-$–N; amendment = 6.6 μg l^{-1} of $^{15}NO_3^-$–N) and the bromide concentration was elevated from a mean of 0.05 mg Br l^{-1} to a mean of 0.75 mg Br l^{-1}. Following the amendment, the solution was injected (pushed) back into the same section of the well. Prior to amendments, we collected background water and gas samples.

During the incubation we collected 30 ml gas and 25 ml water samples every 30 min for a minimum of 3 h. Prior to each sampling we purged wells for 4 min (pumping rate = 1 l min^{-1}) to remove water from the tubing and the well, and to draw water from the interstitial space of sediments. The hydraulic conductivity of the sediments was high enough (Table 1) that this pumping rate did not alter the

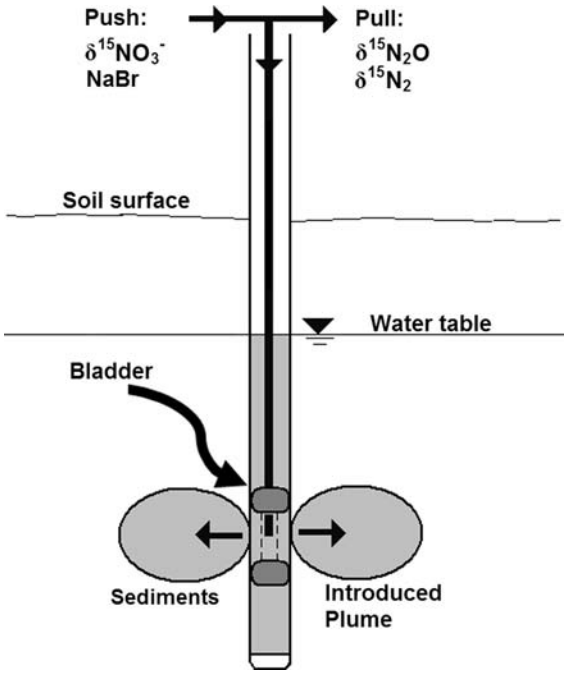

Fig. 2 Diagram of the in situ push–pull $\delta^{15}NO_3^-$ technique. A conservative tracer (NaBr) and $\delta^{15}NO_3^-$ was injected (pushed) into a sealed 20 cm section of the well. During the extraction (pull) phase, gas samples for $\delta^{15}N_2O$ and $\delta^{15}N_2$ and water samples for NaBr and $\delta^{15}NO_3^-$ analysis were collected

hydraulic head in the wells. After return to the lab, gas samples were extracted from the water by headspace equilibration with helium (see method in Jones and Mulholland 1998a) and transferred to evacuated vials. Water samples were filtered and analyzed for nitrate and bromide using the methods previously described. The concentrations and isotopic composition of N_2 and N_2O gases were determined on an isotope ratio mass spectrometer at the University of California Davis Stable Isotope Facility. The ^{15}N:^{14}N ratio was expressed in units of atom % ^{15}N.

Push–pull calculations

To calculate denitrification rate from the push–pull method it is necessary to account for both the dilution of substrate ($^{15}NO_3^-$) and dilution of the end products ($^{15}N_2O$ and $^{15}N_2$). Thus, denitrification rate is calculated from the increase in groundwater dilution corrected $^{15}N_2O$ and $^{15}N_2$ over time. We used Bunsen solubility coefficients ($N_2O = 0.607$ l gas l^{-1} H_2O, $N_2 = 0.015$ l gas l^{-1} H_2O) from Wanninkhof (1992) and Weiss and Price (1980) to calculate the concentrations of N_2O and N_2 in solution. The concentrations of $^{15}N_2O$ and $^{15}N_2$ were calculated by multiplying the concentrations of N_2O and N_2 by the respective atom % ^{15}N. During each sampling interval, the production of $^{15}N_2O$ and $^{15}N_2$ and concentration of $^{15}NO_3^-$ were corrected for dilution using the geometric mean of the decline in bromide concentration. Denitrification rate (R; μg l^{-1} min^{-1}) is the slope of the increase in groundwater dilution-corrected $^{15}N_2O$ and $^{15}N_2$ over time, computed as

$$R = \frac{\left(\frac{^{15}N_{gas_t} - \beta^{15}N_{gas_0}}{^{15}NO_3^-(\%)\beta}\right)}{t} \quad (4)$$

where $^{15}N_{gas_t}$ is the concentration of ^{15}N ($N_2O + N_2$; μg l^{-1}) at time t, $^{15}N_{gas_0}$ is the concentration of gaseous ^{15}N (μg l^{-1}) at the beginning of each assay, $^{15}NO_3^-$ (%) is the percent $^{15}NO_3^-$ added to the well at the start, β is the geometric mean of dilution (D), and t is the incubation time (min).

The dilution of $^{15}NO_3^-$, $^{15}N_2O$, and $^{15}N_2$ in the well from subsurface water flow was calculated from the decline in the conservative tracer as

$$D = \frac{Br_t}{Br_0} \quad (5)$$

where Br_t is the bromide concentration (μg l^{-1}) at time t, and Br_0 is the initial bromide concentration (μg l^{-1}). Denitrification rate was expressed per mass of sediment, and on an areal basis using bulk density and sample depth values of 1.15 g cm^{-3} and 0.2 m (spacing of bladders), respectively. For the areal expression of denitrification, using the spacing of bladders provided a conservative estimate of the overall rate.

The large concentration of $^{14}N_2$ in the atmosphere is a potential source of interference in $^{15}N_2$ studies. The push–pull technique uses suspended bladders beneath the water surface, which prevents interference from atmospheric nitrogen. To ensure that our sample vials were gas-tight and that measured $^{15}N_2$ concentration was not diluted due to $^{14}N_2$ contamination from the atmosphere, we calculated the expected mass of N_2 if there was no air contamination (assuming that the water samples were at equilibrium N_2 levels with the atmosphere) and then used the expected and measured N_2 concentrations to calculate the percent of N_2 in the samples gained

Table 1 Hydraulic gradient, hydraulic conductivity, and subsurface flow rate (mean ± SE) for Islands I and II

Site	Hydraulic gradient ($\Delta h/\Delta l$)	Hydraulic conductivity (m day^{-1})	Subsurface flow rate (m day^{-1})
Island I	0.036 ± 0.007	6.2 ± 1.0	0.33 ± 0.05
Island II	0.040 ± 0.010	4.1 ± 0.7	0.32 ± 0.06

from the atmosphere. We did not use samples that contained greater than 1% N_2 contamination.

Data analysis

Simple linear regression was used to analyze relationships between mean river stage and mean water table height. Change in hyporheic chemistry along well transects was tested using one-way Analysis of Variance (ANOVA). If a significant difference was found ($P < 0.05$), we used Tukey's test to determine which wells were significantly different ($P < 0.05$). Two-way ANOVA was used to determine temporal variations in hyporheic solute or gas concentrations along each well transect.

Analysis of subsurface hydrology and capillary rise

We evaluated the fate of nitrogen in the hyporheic zone by addressing the relative importance of denitrification versus plant uptake. Substantial plant uptake of hyporheic ^{15}N labeled nitrogen was reported at our study sites by Lizzuso et al. (in press). Saturation of the rooting zone as a mechanism for nitrate loss was modeled from measurements of subsurface flow rate and hyporheic water height. To characterize fluctuations in water table height two wells at each island were instrumented with Campbell Scientific CR10X dataloggers and pressure transducers that recorded water table height every 15 min in 2003 and 2005. Water table height measured by the dataloggers was calibrated with biweekly measurements of well water height. The direction and slope of subsurface water flow was then mapped using the height of hyporheic water along the well transects, and in the wells positioned lateral to each well transect. The response of water table height relative to river stage was determined from mean daily river stage data from the U.S Geological Survey (USGS) Tanana River gauging station (#15485500) at Fairbanks, Alaska available from 1990 to 2005. To determine the temporal variation in sediment saturation, we modeled mean hyporheic water height from 1990 to 2005 using the linear relationship between floodplain water table height and river stage. The height of capillary rise above the water table was calculated as a function of soil pore size, with fine soil particles exerting the most control over capillary rise. Using soil sieves we measured the effective particle size (D_{10}), which is the diameter (mm) of the smallest size fraction that accounts for less than 10% of total soil mass. We then used Hazen's formula (Henry 1995, Das 2002) of capillary rise

$$h_c = \frac{m}{D_{10}} \tag{6}$$

where the mean height of capillary rise is h_c (mm), and m is a constant of 30 mm^2. The rate of capillary rise for sandy soils is approximately 0.5 m day^{-1} (Lu and Likos 2004; assuming capillary rise and vertical hydraulic conductivity values of 0.85 and 0.1 m day^{-1}, respectively). Accordingly, we use a conservative lag period of 2 days for the capillary fringe to respond to changes in water table height.

In order to compare the lateral flux of nitrogen in hyporheic flow with areal measurements of soil nitrogen mineralization (Kielland et al. 2006) we calculated area specific hyporheic nitrogen turnover. Nitrogen turnover was calculated assuming a water depth of 2 m (depth of wells). Nitrogen turnover (F; g N m^{-2} day^{-1}) was calculated as

$$F = (TNz)\eta \tag{7}$$

where T is the hydrologic turnover time (well volume (m^3)/water flux into well (m^3 day^{-1}), N is the mean nitrogen concentration in hyporheic water (g N m^{-3}), z is water depth (2 m), and η is the mean measured porosity (0.54).

Long term patterns in climate and river hydrology

To address the importance of local climate on river discharge and the subsequent effects on hyporheic

biogeochemistry, we analyzed 30 years of river discharge data and 70 years of climate data. Daily air temperature data for Fairbanks were obtained from the University of Alaska Fairbanks Climate Center. Tanana River discharge was measured daily at the USGS gauging station on the Tanana River at Fairbanks. These data were used to evaluate seasonal and interannual patterns in river and hyporheic nitrate concentration and methane partial pressure.

Results

Climate and river hydrology

Discharge of the Tanana River was closely correlated with daily maximum air temperature (Fig. 3a). Maximum river discharge occurred in mid to late July (ca. 1,500 $m^3\ s^{-1}$; Fig. 3b) during the time of high solar radiation and glacial melt. Over the three study years, flooding (>1,500 $m^3\ s^{-1}$) of the floodplain (up to 0.7 m standing water) occurred in July of 2003 and in late June to early July of 2005, and persisted for up to 1 month. However, river discharge was elevated (>1,300 $m^3\ s^{-1}$) from June to August in 2004 and 2005 (Fig. 3b).

Groundwater flowpaths

Water table height decreased with distance from the river (Fig. 4a). The direction of hyporheic water flow closely aligned with the orientation of the hyporheic well transects (Fig. 4b). At Island I and Island II, respectively, hydraulic conductivity averaged 6.2 and 4.1 m day^{-1} (Table 1) and hydraulic gradient averaged 3.6 and 4.0% (Table 1). Hyporheic flow rates averaged 0.3 m day^{-1} at the two islands (Table 1). Subsurface flowpaths along the islands were shortened during peak river stage, when the river channels widened up to 100 m. Consequently, the distance between the first well and the river changed substantially with season, with distances from the aquatic-terrestrial interface ranging from ca. 10 to 100 m depending on river stage.

Spatial patterns in hyporheic chemistry

Dissolved oxygen concentration was low in all wells, averaging 2.3 $mgO_2\ l^{-1}$ at Island I and 0.9 $mgO_2\ l^{-1}$ at Island II (Fig. 5). Oxygen concentration did not significantly change along the well transect across Island I ($P = 0.53$), whereas across Island II, oxygen concentration was higher in the well closest to the river ($P < 0.05$), and tended to decline with distance from the river (Fig. 5).

Similar to oxygen, substantial change in hyporheic nitrate concentration occurred as river water entered the hyporheic zone. The concentration of nitrate in river water was on average 3-fold greater than the concentration in hyporheic water ($P < 0.05$; Fig. 6a–f). Approximately 60–80% of river water nitrate was removed during the first 50 m of the flowpaths, and up to a further 20% between the first and second wells. Following this initial decline at the river-

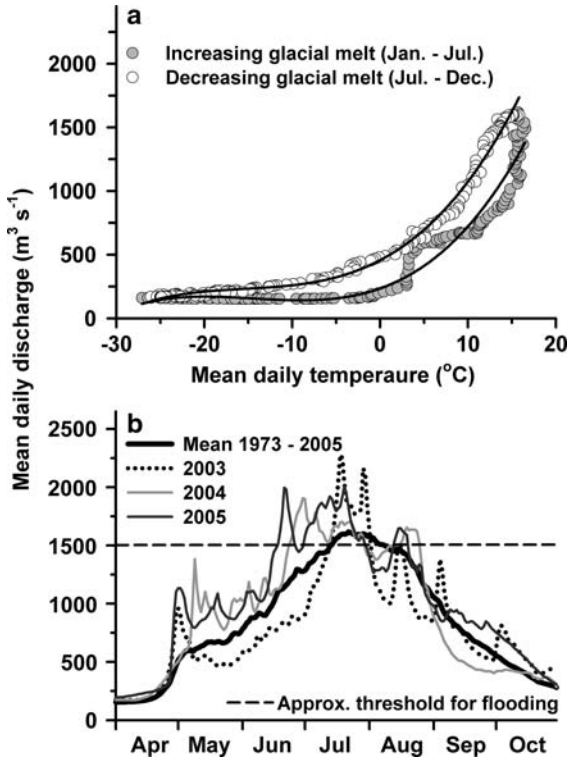

Fig. 3 Cubic regression between mean daily air temperature and mean daily river discharge from 1973 to 2005 (**a**). Trends in river discharge: with increasing air temperature from January to mid-July ($y = 234.79 + 24.45 * x + 1.95 * x^2 + 0.046 * x^3$; $r^2 = 0.95$; $P \leq 0.05$), and decreasing air temperature from mid-July to December ($y = 456.43 + 36.18 * x + 2.10 * x^2 + 0.045 * x^3$; $r^2 = 0.99$; $P \leq 0.05$). Temporal variation in river discharge for the long term mean 1973–2005, and three study years (**b**). Discharge data are from the USGS gauging station (#15485500) located at Fairbanks, Alaska

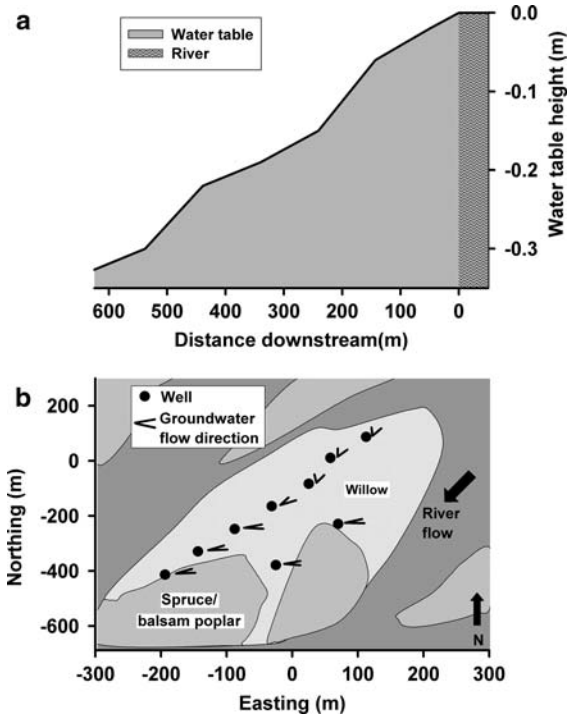

Fig. 4 Cross-sectional view of water table height along the well transect at Island II during peak river flow (18th July 2005; **a**). The river is 0 m downstream, and the soil surface is 0 m on the y-axis. (**b**) Shows the location of hyporheic wells (●) at Island II on the Tanana River. Arrows represent dominant flow vectors along subsurface flowpaths calculated from the change is hydraulic head in wells

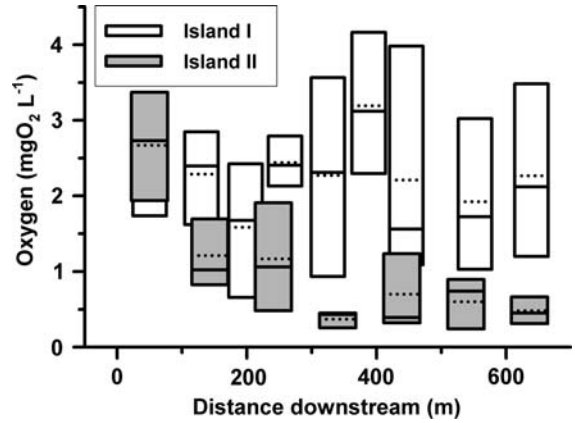

Fig. 5 Longitudinal patterns of oxygen concentration at Island I and Island II. The solid center line, broken line, box extent and error bars circles denote the median, mean, 25th and 75th, 10th and 90th percentiles, respectively

sediment interface, nitrate concentration was fairly stable along the remaining flowpaths ($P > 0.05$; Fig. 6a–f). DON was approximately 2-fold greater in river water than hyporheic water, and did not change significantly along the well transects ($P > 0.05$). In contrast to nitrate, chloride concentration did not change as river water entered the hyporheic zone and behaved conservatively along the flowpaths ($P > 0.05$; Fig. 7a and b). In river and hyporheic water, cation concentrations followed the pattern of Ca > Mg > Na > K. The relative composition of base cations in hyporheic water aligned along the calcium and magnesium axes, with river water as one of the source waters (Fig. 8). The chemical composition of river water was similar to the cation composition from water extractions of sediments, with calcium and magnesium accounting for ca. 67 and 25% of cation composition, respectively. With further contact time between hyporheic water and sediments, magnesium accounted for up to 60% of the cations. As river water entered the hyporheic zone, base cation, bicarbonate, and hydrogen ion concentrations increased significantly ($P < 0.05$; Table 2; Fig. 8).

Hyporheic water was always supersaturated in carbon dioxide, with carbon dioxide averaging 53-fold greater than atmospheric equilibrium (Fig. 9a), and ranging from 5,197 to 45,768 ppmv at Island I and 1,510 to 55,149 ppmv at Island II. The partial pressure of carbon dioxide increased along the well flowpaths at both islands ($P < 0.05$; Fig. 9a). In contrast to carbon dioxide, the partial pressure of methane did not increase along the flowpaths ($P > 0.05$), but instead was elevated in hotspots with supersaturation ranging from 100 to 2,000 times greater than atmospheric equilibrium (Fig. 9b).

Hyporheic chemistry at the transitional boundary between willow and alder stands at Island II was markedly different than hyporheic chemistry in the wells located on younger terraces, which were colonized primarily with willow (Table 2). Of particular interest was the high methane partial pressure (73,344 ± 14,856 ppmv) measured at Island II transitional wells (Table 2). This area of the floodplain was inundated with water for much of the summer, resulting in prolonged soil saturation and consistently low oxygen concentration (0.5 ± 0.1 $mgO_2\ l^{-1}$; Table 3). Methane concentration at the transitional boundary between willow and alder stands at Island II averaged 1.3 mg C l^{-1}, a sizable concentration compared with DOC (4.0 mg C l^{-1}; Tables 2 and 3).

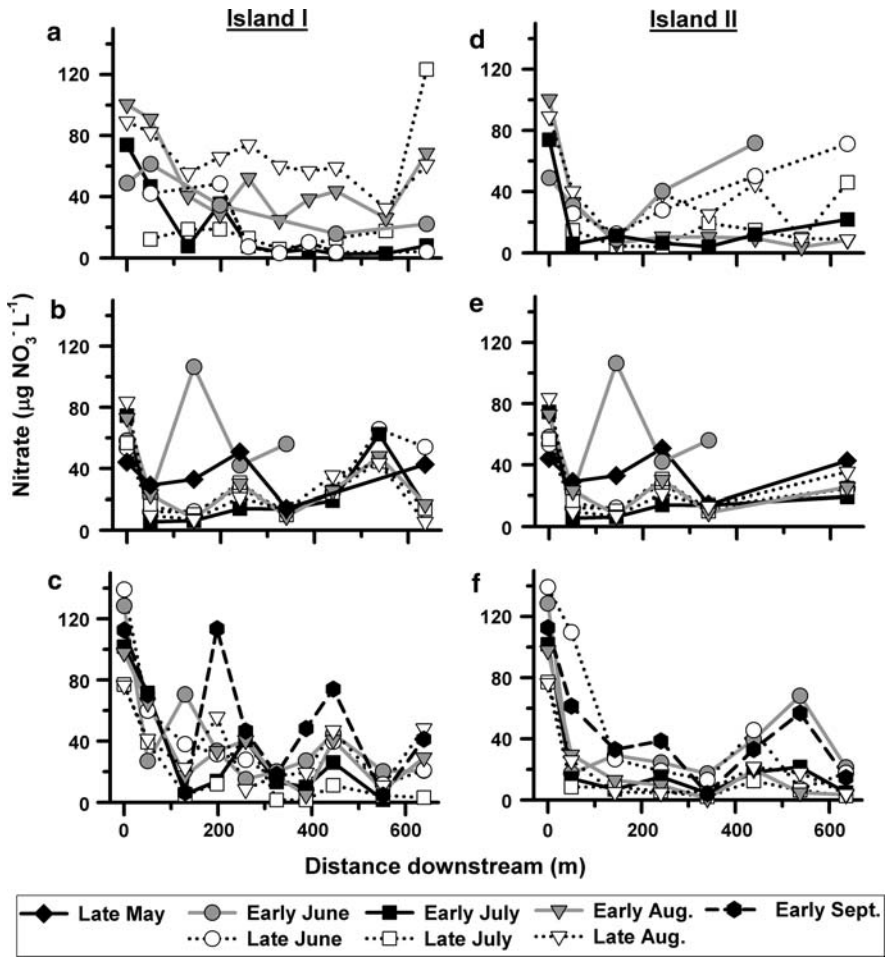

Fig. 6 Longitudinal decline in nitrate concentration along hyporheic flowpaths at Island I (**a**–**c**) and Island II (**d**–**f**) for 3 years: 2003 (top panels), 2004 (middle panels) and 2005 (bottom panels). The river is 0 m downstream

Using the ratio of CH_4 (mg C l^{-1}) to CO_2 (mg C l^{-1}) as an index of anaerobic metabolism (Dahm et al. 1991; Jones and Mulholland 1998b), anaerobic metabolism in transition wells was, on average, 60 times higher (CH_4:CO_2 = 0.15) than in the open willow stands (CH_4:CO_2 = 0.0024) on Island II, and on average 145 times higher than open willow stands on Island I (CH_4:CO_2 = 0.0010; $P < 0.05$; Table 3).

Subsurface hydrology and nitrogen losses

We found a strong positive linear relationship between mean river stage and mean water table height ($r^2 = 0.93$, $P < 0.05$), with an average 1 m change in river height resulting in an average water table height increase of 0.82 m with little lag time (<1 day; Fig. 10a). The mean water table height (1990–2005) was above the mean rooting depth for floodplain willow (0.75 m; Lisuzzo et al. in press) for approximately 2 months (mid-June to August; Fig. 10b). In addition, modelled capillary rise was an additional 0.72 ± 0.26 m, which increased saturation of the rooting zone by approximately 90 days (Fig. 10b).

Loss of nitrate via denitrification was highly variable among wells, ranging from 2 to 30 mg N kg sediment^{-1} day^{-1} at Island I and 3–25 mg N kg sediment^{-1} day^{-1} at Island II (Table 3). Subsurface flux of nitrogen through the top 2 m of sediment averaged 0.41 ± 0.05 g NO_3^-–N m^{-2} day^{-1}, 0.22 ± 0.03 g NH_4^+–N m^{-2} day^{-1} and 3.6 ± 1.5 g DON m^{-2} day^{-1}. Areal measurements of denitrification rate averaged 1.98 ± 0.46 g N m^{-2} day^{-1}.

Temporal variation in hyporheic chemistry

The influence of river stage on hyporheic chemistry was examined by analyzing temporal variations in hyporheic nitrate concentration, DOC concentration,

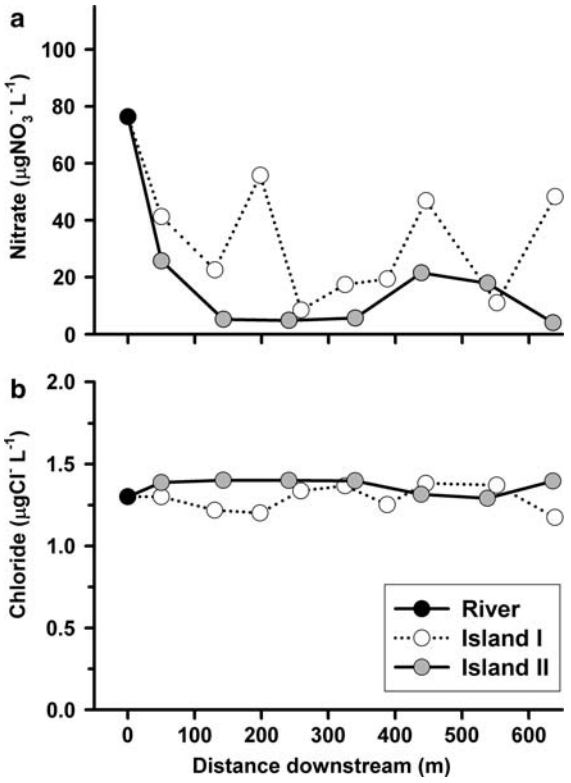

Fig. 7 Longitudinal decline in nitrate concentration (**a**) compared to the conservative tracer chloride (**b**). The example is from Island I and Island II during peak river stage in 2005. The river is 0 m downstream

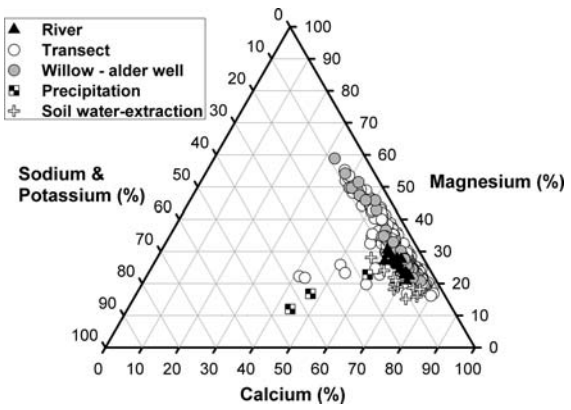

Fig. 8 Ternary plot of base cation chemistry in river water, hyporheic water along the well transects, hyporheic water in the willow-alder transitional wells, soil water-extractions, and precipitation

and methane partial pressure relative to change in river flow. During peak river stage (July–early August), mean hyporheic nitrate concentration at Island II decreased 2-fold compared with early summer (June) ($P < 0.05$; Fig. 11). In addition, methane partial pressure was one to two orders of magnitude greater during peak flow in 2004 and 2005 than during base flow ($P < 0.05$; Fig. 11). The saturation of surface sediment was prolonged throughout the summer in the 2004 and 2005 study years (warm and dry summers), whereas in 2003 (cooler and wetter summer) the floodplain was relatively dry, except for brief flooding in July (Fig. 3). Associated with this increased saturation in 2004 and 2005, mean methane partial pressure was 3-fold greater in 2004 and 2005 than in 2003 ($P < 0.05$; Fig. 11).

Discussion

Hyporheic zone hydrology and nitrogen transformation

The height of the water table on the Tanana River floodplain was closely coupled to river stage, which in turn was controlled by rate of glacial melt due to increased ambient air temperature (Fig. 3a). Horizontal subsurface flow was slow (ca. 3 m day^{-1}) compared with the rapid (<1 day) vertical changes in water table height, suggesting that movement of river water and nutrients through the subsurface was more likely dominated by vertical changes in water table height in response to river stage.

Hydrologic exchange between well oxygenated, nutrient rich surface water and metabolically active alluvial sediment is important for nutrient retention (Jones et al. 1995b, Pinay et al. 1995) and floodplain productivity (Schade et al. 2002). Surface water of the Tanana River is richer in nitrate and DOC relative to the hyporheic zone and thus represents a potential source of nutrients. There are two transfer mechanisms that drive river water intrusion and mixing in the hyporheic zone of these islands, (1) episodic inundation of the floodplain (June–August), and (2) constant horizontal flow. The presence of river water in the hyporheic zone of these islands is supported by (1) the conservative nature of chloride between the river and wells (Fig. 7b), (2) the alignment of well water and river water along the same calcium and magnesium axes (Fig. 8), and (3) the similar base cation composition of river water and the water

Table 2 Ion concentrations and partial pressure of gases for the Tanana River, hyporheic well transects (Island I and II) and the willow-alder transitional wells (Mean ± SE; n.d. = no data)

	Site				
	River	Island I transect wells	Island II transect wells	Island I transitional well	Island II transitional wells
pH	7.9 ± 0.04	7.7 ± 0.03	7.8 ± 0.03	7.7 ± 0.4	7.77 ± 0.07
Conductivity ($\mu s\ cm^{-1}$)	246 ± 7	779 ± 16	651 ± 11	671 ± 18	649 ± 11
Na^+ ($mg\ l^{-1}$)	4.0 ± 0.1	7.7 ± 0.4	7.48 ± 0.5	5.9 ± 0.4	6.0 ± 0.1
Mg^{2+} ($mg\ l^{-1}$)	8.6 ± 0.3	29.6 ± 1.1	23.0 ± 0.6	23.8 ± 1.3	23.8 ± 0.7
K^+ ($mg\ l^{-1}$)	1.7 ± 0.1	4.6 ± 0.4	4.0 ± 0.2	3.2 ± 0.3	4.1 ± 0.2
Ca^{2+} ($mg\ l^{-1}$)	37.0 ± 1.3	135 ± 6	83.3 ± 3.3	104 ± 10	77.4 ± 4.2
NH_4^+ ($\mu g\ N\ l^{-1}$)	12.4 ± 2.6	14.6 ± 1.6	15.3 ± 1.7	20.2 ± 10.7	32.0 ± 4.3
HCO_3^- ($mg\ l^{-1}$)	91.1 ± 8.6	328 ± 25	349 ± 15	304 ± 23	369 ± 18
SO_4^- ($mg\ l^{-1}$)	16.2 ± 1.8	53.6 ± 2.6	22.8 ± 1.7	35.7 ± 2.3	11.4 ± 2.6
NO_3^- ($\mu g\ N\ l^{-1}$)	86.5 ± 6.3	29.1 ± 1.7	24.3 ± 2.0	37.4 ± 7.5	14.2 ± 4.6
DON ($\mu g\ N\ l^{-1}$)	362 ± 42	228 ± 10	240 ± 8	239 ± 33	309 ± 30
DOC ($mg\ C\ l^{-1}$)	4.0 ± 0.9	3.8 ± 0.7	2.7 ± 0.08	2.7 ± 0.4	4.0 ± 0.3
SUVA ($l\ mg^{-1}\ m^{-1}$)	3.8 ± 0.6	1.8 ± 0.2	1.8 ± 0.1	1.7 ± 0.4	2.2 ± 0.13
DO ($mgO_2\ l^{-1}$)	n.d.	2.3 ± 0.2	1.5 ± 0.2	2.0 ± 0.4	0.53 ± 0.05
N_2O (ppmv)	n.d	0.51 ± 0.1	1.2 ± 0.6	0.5 ± 0.1	2.6 ± 2.0
CO_2 (ppmv)	1,876 ± 175	19,752 ± 536	20,585 ± 859	15,871 ± 1547	22,080 ± 1572
CH_4 (ppmv)	128 ± 19	364 ± 134	1,450 ± 371	85 ± 26	73,344 ± 14856

extractions of sediments (Fig. 8). Although the river water and water extractions of sediments contained less exchangeable cations than the well water (Fig. 8), this is likely due to little contact time with sediments (extractions ran for ca. 24 h). In the case of well water, as river water enters the hyporheic zone the increased contact time with reactive glacial deposits, and production of carbonic acid from heterotrophic and autotrophic (root) respiration, can collectively increase the solubility of base cations and bicarbonate anions in solution (Faure 1998).

Spatial differences in subsurface nitrogen chemistry were most pronounced at the river-sediment interface, with rapid removal of nitrate (60–80% reduction) during the first 50 m of hyporheic flowpaths. Strong removal of nitrate at the river-sediment interface was most likely attributable to denitrification rather than plant uptake as this region of the floodplain was sparsely vegetated. This rapid loss is similar to previous findings that have shown that the aquatic-terrestrial interface is an important control point for nitrogen retention (Holmes et al. 1996; Hedin et al. 1998; Devito et al. 2000). Rapid denitrification at the river-sediment interface is likely driven by the supply of electron acceptors and donors from surface water, and the sharp oxygen gradient as surface water enters the hyporheic zone (Duff and Triska 1990; Vervier et al. 1993; Baker et al. 1999; Baker and Vervier 2004). Apart from the initial decline in nitrate concentrations between the river and the first hyporheic wells, nitrate concentrations were relatively constant along the remaining flowpaths. This consistency suggests that the rate of denitrification, the process that largely governs the retention of hyporheic nitrate at these islands, is limited by the supply of nitrate and/or DOC from the river, mineralization, and nitrification.

In contrast to the lack of spatial variation, the concentration of nitrate in the hyporheic zone varied temporally with change in river discharge. As river stage increased (June to early August), hyporheic nitrate concentration at Island II decreased 2-fold. This decline in nitrate concentration may be a biologically mediated loss (i.e., denitrification and/or plant uptake) associated with increased saturation of surface sediment. Alternatively, the decline may

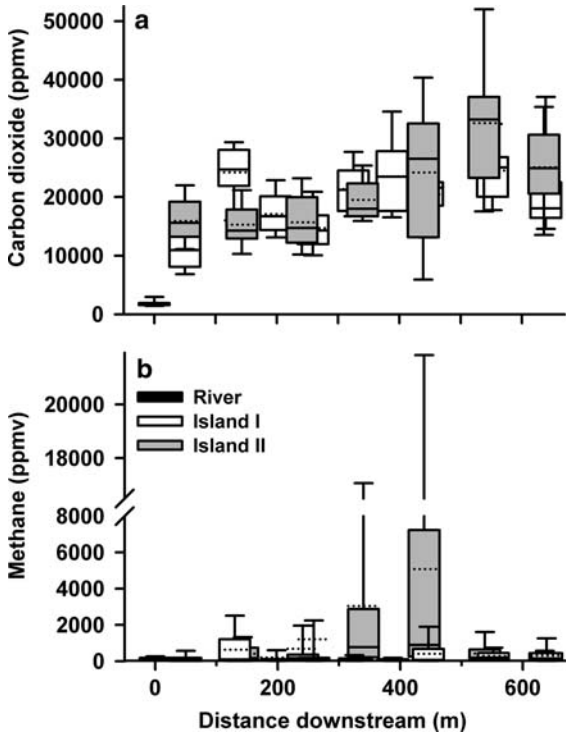

Fig. 9 Longitudinal patterns in the partial pressure of carbon dioxide (**a**) and methane (**b**) at Island I and Island II. The river is 0 m downstream

be hydrologic in that as the water table increased in height, the vertical transfer of water may transport deeper hyporheic water, which is depleted in nitrate, into the well sampling profile. On the trailing limb of peak river flow, hyporheic nitrate concentrations increased as water receded during late August. During flood stage, Island II had standing water from the river, which had a higher nitrate concentration than the hyporheic water. As river stage declined, this nitrate-rich surface water would percolate into the hyporheic zone and serve as a pulse of nitrate to the subsurface. Moreover, as a consequence of flooding, the hyporheic zone likely has periods of hydrologic exchange with surface waters.

Denitrification rates measured in our study were similar to those in a nitrogen-limited Sonoran desert stream (Holmes et al. 1996), and studies that also used an in situ push-pull method on the Garonne River (Baker and Vervier 2004) and in riparian zones in Rhode Island (Addy et al. 2002). Our denitrification data suggest that in the boreal forest, floodplain sediments have a large capacity for denitrification during peak river stage in the summer. Moreover, denitrification rate (1.98 ± 0.46 g N m^{-2} day^{-1}) in hyporheic water beneath early succession willow stands of the Tanana River is approximately two orders of magnitude greater than plant uptake (0.013 g N m^{-2} day^{-1}; Lizzuso et al. in press), and appears to be the dominant pathway of nitrogen removal.

Hyporheic flow appears to be an important mechanism of nitrogen supply to willow stands on the Tanana River floodplain. Using injections of ^{15}N labeled nitrogen into buried flowboxes, Lizzuso et al. (in press) found substantial uptake of hyporheic nitrogen in willow stands on the Tanana River. We found that horizontal fluxes of dissolved nitrogen (averaging 0.6 g DIN m^{-2} day^{-1} and 3.6 g DONm^{-2} day^{-1}) through the top 2 m of sediment far exceed nitrogen inputs from soil organic matter turnover (0.0028 g N m^{-2} day^{-1}; Kielland et al. 2006), nitrogen fixation (0.00027 g N m^{-2} day^{-1}; Klingensmith and Van Cleve 1993) and atmospheric

Table 3 Concentrations of hyporheic oxygen and dissolved organic carbon (mean ± SE), indices of hyporheic anaerobic respiration ($CH4:CO_2$; mean ± SE), and denitrification rates in hyporheic sediments (mean ± SE), for the well transects (Island I and II) and wells at the willow-alder transitional wells (Island I T and Island II T)

	Site			
	Island I transect wells	Island II transect wells	Island I transitional well	Island II transitional wells
O_2 (mgO_2 l^{-1})	2.3 ± 0.2	1.5 ± 0.2	2 ± 0.4	0.5 ± 0.1
DOC (mg C l^{-1})	3.8 ± 0.7	2.7 ± 0.1	2.7 ± 0.4	4 ± 0.3
CH_4 (mg C l^{-1}):CO_2 (mg C l^{-1})	0.001 ± 0.001	0.003 ± 0.001	0.001 ± 0.000	0.146 ± 0.032
Denitrification (mg N kg^{-1} day^{-1})	7.8 ± 2.4	10.4 ± 3.9	nd	nd

Denitrification rates are from July to September in 2005

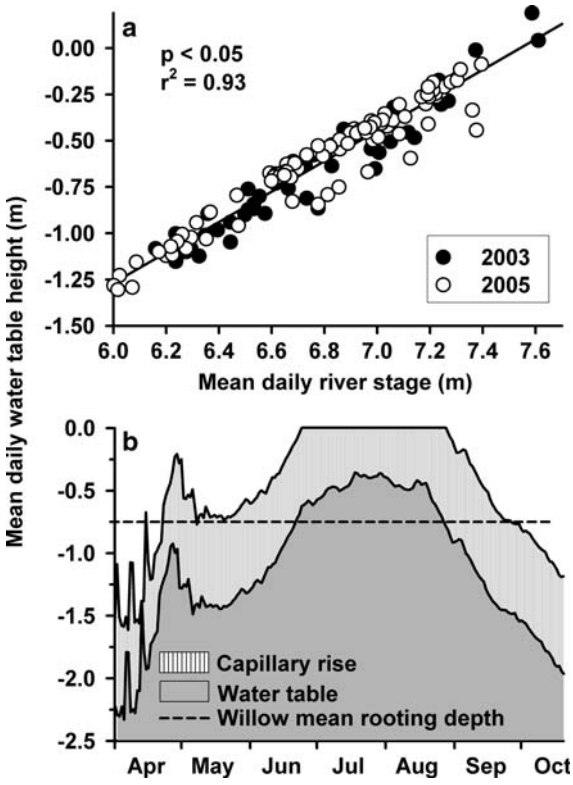

Fig. 10 Relationship between mean water table height and mean daily river stage (**a**) for both islands. Line indicates statistically significant regression at $P < 0.05$ and $r^2 = 0.93$, Slope = 0.82 and y = 0.8227x + (−6.2044). Predicted mean water table height using the regression relationship in (**a**) and river stage data (mean river stage from 1990 to 2005) from Fairbanks USGS gauging station (**b**). Dashed horizontal line denotes mean willow rooting depth

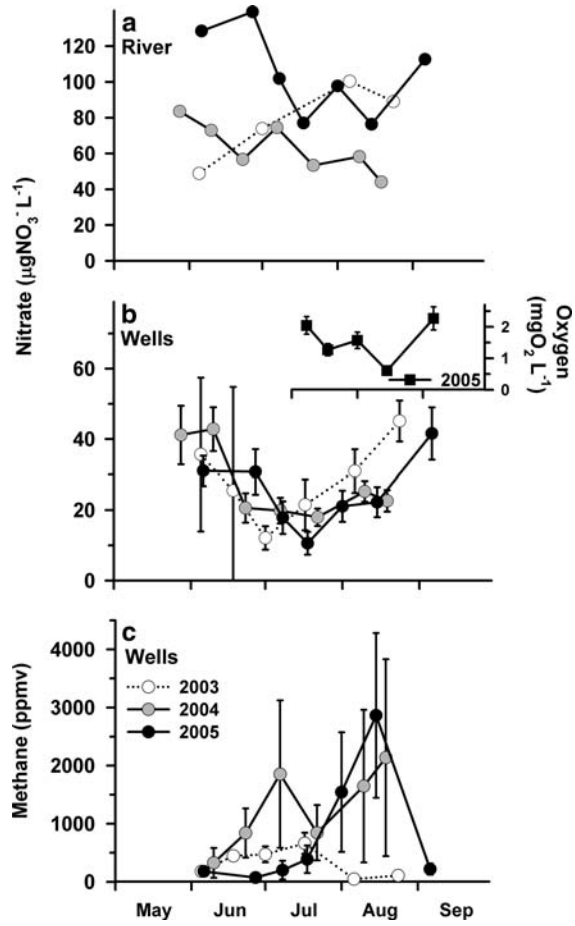

Fig. 11 Temporal variations in river nitrate concentration (**a**), hyporheic oxygen and nitrate concentration (mean ± SE; **b**), and methane partial pressure (mean ± SE; **c**) at Island II over the three study years

deposition (0.00025 mg N m^{-2} day^{-1}; National Atmospheric Deposition Program). Vertical fluctuations in water table height dominate the movement of water in the hyporheic zone, and represent a large pool of nitrate (sediments on the Tanana River floodplain can be >100 m thick; Péwé and Reger 1983) that could supply nitrogen to microbes and vegetation. The capillary fringe is within the rooting zone for early successional floodplain vegetation and may further enhance hydrologic connectivity between hyporheic water and the rooting zone of vegetation. Our results are comparable to capillary rise measurements of 1.0–1.5 m for weakly compacted alluvial sandy loams (Chubarova 1972), and reports of capillary rise to 0.1–0.5 m below the soil surface in open willow stands on the Tanana River floodplain (Viereck et al. 1993b).

Subsurface methane and carbon dioxide

Although at both islands carbon dioxide was the dominant gas in solution, methane comprised a significant proportion of respiratory gases at Island II. Hotspots of methane production at Island II occurred where mean oxygen concentration had fallen below 0.5 mgO_2 l^{-1}. The partial pressure of methane was greatest in hyporheic water at the transitional boundary between willow and alder stands at Island II, where subsurface flow through a denser root mass, converged with sediment that was covered with standing water for prolonged periods. At this boundary, methanogenesis was a sizable component of subsurface metabolism based on the CH_4:CO_2 ratio and composed one-third of the

dissolved carbon pool in the sediment when summed with DOC. To test whether upwelling of deeper groundwater could account for the high methane partial pressure at Island II transitional wells, we compared base cation concentrations among the wells. The concentration of calcium and magnesium did not differ significantly between the well transects and transitional wells (Fig. 8) indicating that spatial differences in hyporheic biogeochemistry were not driven by source waters other than the river. Alternatively, differences in hyporheic biogeochemistry in the transitional wells may result from hydrologic flow through later successional stands, such as alder, and balsam poplar. In comparison to open willow stands, soils in these stands have a developed organic horizon and higher nitrate concentration (Viereck et al. 1993b, Kielland et al. 2006), which may serve as a source of DOC and nitrate for hyporheic metabolism and warrants further research.

Climate, river hydrology and hyporheic chemistry

Hydrology of glacially fed rivers is largely governed by regional climate. During high river stage in the summer, the net flow of water is from the surface channel to the hyporheic zone which functions as a sink for nitrogen. Hyporheic chemistry was coupled to periods of flooding that saturated the sediment profile and altered the oxidation state of hyporheic water. We found that denitrification was an important sink for nitrogen in the hyporheic zone and was most pronounced at the river-stream interface. Methane partial pressure was particularly high during years with prolonged soil saturation throughout the summer, suggesting that a high and stable river stage promotes lower redox potential of floodplain sediment and increases the rate of anaerobic respiration. Similarly, we suggest that the supply of hyporheic nutrients to floodplain vegetation will be greatest during summers with highest river discharge. Indeed as interior Alaska continues to warm (Hinzman et al. 2006), associated changes in the hydrologic regime of the Tanana River have the potential to increase the productivity of early successional floodplain vegetation, and enhance anaerobic metabolism in the hyporheic zone.

Acknowledgements Many thanks to Nicolas Lisuzzo, Karl Olson, Jessica Eichmiller, Kelly Balcarczyk, Emma Betts and Jon O'Donnell for their assistance in the field and laboratory. We also thank Richard Boone, who provided valuable comments on the research and manuscript. Thanks to Larry Hinzman for help with the experimental design and well installation. This work was supported by grants from the Andrew W. Mellon Foundation and the Bonanza Creek LTER Program (funded jointly by NSF grant DEB-0423442 and USDA Forest Service, Pacific Northwest Research Station grant PNW01-JV11261952-231). Additional assistance was provided by the Cooperative Institute for Arctic Research, the Center for Global Change, and University of Alaska Fairbanks.

References

Addy K, Kellogg DQ, Gold AJ, Groffman PM, Ferendo G, Sawyer C (2002) In situ push–pull method to determine ground water denitrification in riparian zones. J Environ Qual 31:1017–1024

Anderson GS (1970) Hydrologic Reconnaisance of the Tanana River Basin, Central Alaska. USGS. Hydrological Investigations HA-319 Tanana Geology

Arendt AA, Echelmeyer KA, Harrison WD, Lingle CS, Valentine VB (2002) Rapid wastage of Alaska glaciers and their contribution to rising sea level. Science 297:382–386

Baker MA, Vervier P (2004) Hydrological variability, organic matter supply and denitrification in the Garonne River ecosystem. Freshw Biol 49:181–190

Baker MA, Dahm CN, Valett HM (1999) Acetate retention and metabolism in the hyporheic zone of a mountain stream. Limnol Oceanogr 44:1530–1539

Boulton AJ, Findlay S, Marmonier P, Stanley EH, Valett HM (1998) The functional significance of the hyporheic zone in streams and rivers. Annu Rev Ecol Syst 29:59–81

Chubarova NP (1972) Computation of the height of capillary rise of water in different genetic types of bound soils. Soil Mech Found Eng 9:25–27

Dahm CN, Carr DL, Coleman RL (1991) Anaerobic carbon cycling in stream ecosystem. Int Ver Theor Angew Limnol Verh 24:1600–1604

Dahm CN, Grimm NB, Marmonier P, Valett HM, Vervier P (1998) Nutrient dynamics at the interface between surface waters and groundwaters. Freshw Biol 40:427–451

Das BM (2002) Principles of geotechnical engineering, 5th edn. Brooks/Cole, Pacific Grove, California

Devito KJ, Fitzgerald D, Hill AR, Aravena R (2000) Nitrate dynamics in relation to lithology and hydrologic flow path in a river riparian zone. J Environ Qual 29:1075–1084

Duff JH, Triska FJ (1990) Denitrification in sediments from the hyporheic zone adjacent to a small forested stream. Can J Fish Aquat Sci 47:1140–1147

Duff JH, Triska FJ (2000) Nitrogen biogeochemistry and surface-subsurface exchange in streams. In: Jones JB Jr, Mulholland PJ (eds) Streams and ground waters. Academic Press, San Diego

Faure G (1998) Principles and applications of geochemistry. Prentice Hall, New Jersey

Findley S (1995) Importance of surface-subsurface exchange in stream ecosystems: the hyporheic zone. Limnol Oceanogr 40:150–164

Freeze RA, Cherry JA (1979) Groundwater. Prentice Hall, Englewood Cliffs

Grimm NB, Fisher SG (1984) Exchange between surface and interstitial water: implications for stream metabolism and nutrient cycling. Hydrobiologia 111:219–228

Hedin LO, Von Fisher JC, Ostrom NE, Kennedy BP, Brown MG, Robertson GP (1998) Thermodynamic constraints on nitrogen transformations and other biogeochemical processes at soil-stream interfaces. Ecology 79:684–703

Henry KS (1995) The use of geosynthetic capillary barriers to reduce moisture migration in soils. Geosynth Int 2:883–888

Hill AR (2000) Stream chemistry and riparian zones. In: Jones JB Jr, Mulholland PJ (eds) Streams and ground waters. Academic Press, San Diego

Hill AR, Devito KJ, Campagnolo S, Sanmugadas K (2000) Subsurface denitrification in a forest riparian zone: interactions between hydrology and supplies of nitrate and organic carbon. Biogeochemistry 51:193–223

Hinzman LD, Bettez ND, Bolton RW, Chapin FS, Dyurgerov MB, Fastie CL, Griffith B, Hollister RD, Hope A, Huntington HP, Jensen AM, Jia GJ, Jorgenson T, Kane DL, Klein DR, Kofinas G, Lynch AH, Lloyd AH, McGuire D, Nelson FE, Oechel WC, Osterkamp TE, Racine CH, Romanovsky VE, Stone RS, Stow DA, Sturm M, Tweedie CE, Vourlitis GL, Walker MD, Walker DA, Webber PJ, Welker JM, Winker KS, Yoshikawa K (2005) Evidence and implications of recent climate change in northern Alaska and other arctic regions. Clim Change 72:251–298

Hinzman LD, Viereck LA, Adams PC, Romanovsky VE, Yoshikawa K (2006) Climate and permafrost dynamics in the Alaskan boreal forest. In: Chapin III FS, Oswold MW, Van Cleve K, Viereck LA, Verbyla DL (eds) Alaska's changing boreal forest. Oxford University Press, New York

Holmes RB, Jones JB Jr, Fisher SG, Grimm NB (1996) Denitrification in a nitrogen-limited stream ecosystem. Biogeochemistry 33:125–146

Jones JB Jr, Holmes RM (1996) Surface-subsurface interactions in stream ecosystems. Trends Ecol Evol 11:239–242

Jones JB Jr, Mulholland PJ (1998a) Methane input and evasion in a hardwood forest stream: effects of subsurface flow from shallow and deep flowpaths. Limnol Oceanogr 43:1243–1250

Jones JB Jr, Mulholland PJ (1998b) Influence of drainage basin topography and elevation on carbon dioxide and methane supersaturation of stream water. Biogeochemistry 40:57–72

Jones JB Jr, Fisher SG, Grimm NB (1995a) Nitrification in the hyporheic zone of a desert stream ecosystem. J North Am Benthol Soc 14:249–258

Jones JB Jr, Fisher SG, Grimm NB (1995b) Vertical hydrologic exchange and ecosystem metabolism in a Sonoran desert stream. Ecology 76:942–952

Kielland K, Ruess RW, Olson K, Boone RD (2006) Contribution of winter processes to soil nitrogen flux in taiga forest ecosystems. Biogeochemistry 81:349–360

Klingensmith KM, Van Cleve K (1993) Denitrification and nitrogen-fixation in floodplain successional soils along the Tanana River, interior Alaska. Can J Forest Res 23:956–963

Lisuzzo NJ, Kielland K, Jones JB Jr (in press) Hydrologic controls of nitrogen availability in a high-latitude, semi-arid floodplain. Ecoscience

Lowrance R, Todd R, Fail J, Hendrickson OJ, Leonard R, Asmussen L (1984) Riparian forests as nutrient filters in agricultural watersheds. Bioscience 34:374–377

Lu N, Likos WJ (2004) Rate of capillary rise in soil. J Geotech Geoenvion 130:646–650

Malard F, Uehlinger U, Zah R, Tockner K (2006) Flood-pulse and riverscape dynamics in a braided glacial river. Ecology 87:704–716

Meyer JL (1988) Benthic bacterial biomass and production in a blackwater river. Int Ver Theor Angew Limnol Verh 23:1838–1838

Morrice JA, Dahm CN, Valett HM (2000) Terminal electron accepting processes in the alluvial sediments of a headwater stream. J North Am Benthol Soc 19:593–608

Ostrom NE, Hedin LO, von Fischer JC, Robertson GP (2002) Nitrogen transformations and NO_3^- removal at the soil-stream interface: a stable isotope approach. Ecol Appl 12:1027–1043

Parkhurst DL, Appelo CAJ (1999) PHREEQC (Version 2) A computer program for speciation, batch-reaction, one-dimensional transport, and inverse geochemical calculations. www.brr.cr.usgs.gov/projects/GWC_coupled/phreeqc/index.html. Cited 04 Apr 2007. USGS site

Péwé TL, Reger RD (1983) Middle Tanana River Valley. In: Péwé TL, Reger RD (eds) Guidebook 1: Richardson and Glenn highways, Alaska. Alaska division of geological and geophysical surveys

Péwé TL, Bell JW, Forbes RB, Weber FR (1976) Geological map of the Fairbanks D-2 SE quadrangle, Alaska: US Geological Survey miscellaneous investigations series map I, 942

Pinay G, Ruffinoni C, Fabre A (1995) Nitrogen cycling in two riparian forest soils under different geomorphic conditions. Biogeochemistry 4:1–21

Robertson GP, Sollins P, Ellis BG, Lajtha K (1999) Exchangeable ions, pH, and cation exchange capacity. In: Robertson GP, Coleman DC, Bledsoe CS, Sollins P (eds) Standard soil methods for long-term ecological research. Oxford University Press, New York

Sabater S, Butturini A, Clement J, Burt T, Dowrick D, Hefting M, Maître V, Pinay G, Postolache G, Rzepecki M, Sabater F (2003) Nitrogen removal by riparian buffers along a European climatic gradient: patterns and factors of variation. Ecosystems 6:20–30

Schade JD, Marti E, Welter JR, Fisher SG, Grimm NB (2002) Sources of nitrogen to the riparian zone of a desert stream: implications for riparian vegetation and nitrogen retention. Ecosystems 5:68–79

Triska FJ, Kennedy VC, Avanzino RJ, Zellweger GW, Bencala KE (1989) Retention and transport of nutrients in a third-order stream in Northwestern California: hyporheic processes. Ecology 70:1893–1905

Triska FJ, Duff JH, Avanzino RJ (1993) The role of water exchange between a stream channel and its hyporheic zone in nitrogen cycling at the terrestrial-aquatic interface. Hydrobiologia 251:167–184

Vervier P, Dobson M, Pinay G (1993) Role of interaction zones between surface and ground waters in DOC transport and

processing: considerations for river restoration. Freshw Biol 29:273–284

Vidon P, Hill AR (2004) Denitrification and patterns of electron donors and acceptors in eight riparian zones with contrasting hydrogeology. Biogeochemistry 71:259–283

Viereck LA, Van Cleve K, Adams PC, Schlentner PE (1993a) Climate of the Tanana River floodplain near Fairbanks, Alaska. Can J Forest Res 23:899–913

Viereck LA, Dyrness CT, Foote MJ (1993b) An overview of the vegetation and soils of the floodplain ecosystems of the Tanana River, interior Alaska. Can J Forest Res 23:889–898

Wanninkhof R (1992) Relationship between wind speed and gas exchange over the ocean. J Geophys Res 97:7373–7382

Weiss RF, Price BA (1980) Nitrous oxide solubility in water and seawater. Mar Chem 8:347–359

Yarie J, Viereck LA, Van Cleve K, Adams P (1998) Flooding and ecosystem dynamics along the Tanana River. Ecoscience 48:690–695